# DSCC2013-4009

# RELIABLE SENSING OF LEAKS IN PIPELINES

**Dimitris M. Chatzigeorgiou** *
**You Wu**
**Kamal Youcef-Toumi**
Mechatronics Research Laboratory
Department of Mechanical Engineering
Massachusetts Institute of Technology
Cambridge, Massachusetts
{dchatzis, youwu, youcef}@mit.edu

**Rached Ben-Mansour**
Department of Mechanical Engineering
King Fahd Univ. of Petroleum & Minerals
Dhahran, Saudi Arabia
{rmansour@kfupm.edu.sa}

## ABSTRACT

*Leakage is the major factor for unaccounted losses in every pipe network around the world (oil, gas or water). In most cases the deleterious effects associated with the occurrence of leaks may present serious economical and health problems. Therefore, leaks must be quickly detected, located and repaired. Unfortunately, most state of the art leak detection systems have limited applicability, are neither reliable nor robust, while others depend on user experience.*

*In this work we present a new in-pipe leak detection system, PipeGuard. PipeGuard performs autonomous leak detection in pipes and, thus, eliminates the need for user experience. This paper focuses on the detection module and its main characteristics. Detection in based on the presence of a pressure gradient in the neighborhood of the leak. Moreover, the proposed detector can sense leaks at any angle around the circumference of the pipe with only two sensors. We have validated the concepts by building a prototype and evaluated its performance under real conditions in an experimental laboratory setup.*

## INTRODUCTION

Potable water obtained through access of limited water reserves followed by treatment and purification is a critical resource to human society. Failure and inefficiencies in transporting drinking water to its final destination wastes resources and energy. In addition to that, there are thousands of miles of natural gas and oil pipelines around the globe that are poorly maintained. Thus, a significant portion of the total oil and natural gas

production is lost through leakage. This causes among others, threats for humans and damage to the environment.

### Out-of-Pipe Methods

There are various techniques reported in the literature for leak detection [1, 2]. First, leak losses can be estimated from audits. For instance in the water industry, the difference between the amounts of water produced by the water utility and the total amount of water recorded by water usage meters indicates the amount of unaccounted water. While this quantity gives a good indication of the severity of water leakage in a distribution network, metering gives no information about the locations of the leaks.

Acoustic leak detection is normally used not only to identify but also locate leaks. Acoustic methods consist of listening rods or aquaphones. These devices make contact with valves and/or hydrants. Acoustic techniques may also include geophones to listen for leaks on the ground directly above the pipes [2]. Drawbacks of those methods include the necessary experience needed by the operator. The method is not scalable to the network range, since the procedure is very slow.

More sophisticated techniques use acoustic correlation methods, where two sensors are placed on either side of the leak along a pipeline. The sensors bracket the leak and the time lag between the acoustic signals detected by the two sensors is used to identify and locate the leak [3]. This cross-correlation method works well in metal pipes. However, a number of difficulties are encountered in plastic pipes and the effectiveness of the method is doubtful [4, 5].

Finally, several non-acoustic methods like infrared thermog-

raphy, tracer gas technique and ground- penetrating radar (GPR) have been reported in the literature of leak detection [6,7]. Those methods have the advantage of being insensitive to pipe material and operating conditions. Nevertheless, a map of the network is needed, user experience is necessary and the methods are in general slow and tedious.

### In-Pipe Methods

Past experience has shown that in-pipe inspection is more accurate, less sensitive to external noise and also more robust, since the detecting system will come close to the location of the leaks/defects in the pipe. In this section various in-pipe leak detection approaches are reported.

The *Smartball* is a mobile device that can identify and locate small leaks in liquid pipelines larger than 6" in diameter constructed of any pipe material [8]. The free-swimming device consists of a porous foam ball that envelops a watertight, aluminum sphere containing the sensitive acoustic instrumentation.

*Sahara* is able to pinpoint the location and estimate the magnitude of the leak in large diameter water transmission mains of different construction types [9]. Carried by the flow of water, the *Sahara* leak detection system can travel through the pipe. In case of a leak, the exact position is marked on the surface by an operator who is following the device at all times. Both *Smartball* and *Sahara* are passive (not actuated) and cannot actively maneuver inside complicated pipeline configurations. Last, operator experience is needed for signal interpretation and leakage identification and localization.

Our group proposed a passive inspection system for water distribution networks using acoustic methods [10]. This detection system is designed to operate in small pipes (4"). The merits of the in-pipe acoustic leak detection under different boundary conditions are reported in [11, 12].

Under some circumstances it is easier to use remote visual inspection equipment to assess the pipe condition. Different types of robotic crawlers have been developed to navigate inside pipes. Most of these systems utilize four-wheeled platforms, cameras and an umbilical cord for power, communication and control, e.g. the *MRINSPECT* [13]. Schemph et al. report on a long-range, leak-inspection robot that operates in gas-pipelines (the *Explorer robot*) [14]. A human operator controls the robot via wireless RF signals and constantly looks into a camera to search for leaks. Such systems are suitable for gas or empty liquid pipelines (off-line inspection).

In the oil industry several nondestructive testing methods are used to perform pipe inspections. Most systems use Magnetic Flux Leakage (MFL) based detectors and others use Ultrasound Techniques (UT) to search for pipe defects [15]. These methods' performance depends on the pipe material. They are also power demanding, most of the times not suitable for long-range missions and have limited maneuvering capabilities because of their large sizes.

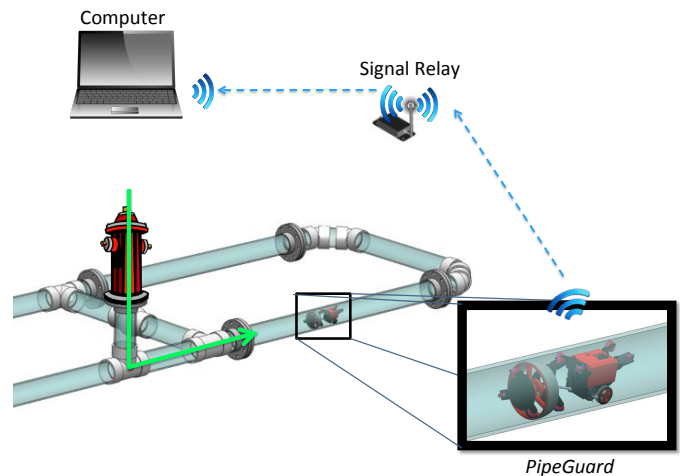In this paper we introduce *PipeGuard*, a new system able to



Figure 1. In-Pipe Inspection using *PipeGuard*. *PipeGuard* travels in the network, searches for and identifies leaks and transmits signals wirelessly via relay stations to a computer.

detect leaks in pipes in a reliable and autonomous fashion (Fig. 1). The idea is that *PipeGuard* is inserted into the network via special insertion points, e.g. fire hydrants in water networks. The system inspects the network and sends signals wirelessly via relay stations to a computer [16]. Leak signals stand out clearly on occurrence of leaks, eliminating the need for user experience. The latter is achieved via a detector that is based on identifying a clear pressure gradient in the vicinity of leaks.

## DETECTION BASED ON PRESSURE GRADIENT

In this section the proposed detection concept and the detector design are discussed. *PipeGuard* is able to detect leaks in a reliable and robust fashion because of the fundamental principle behind detection. More specifically, the detection principle is based on identifying the existence of a localized pressure gradient ($\partial p(r)/\partial r$). This pressure gradient appears in pressurized pipes in the vicinity of leaks and is independent of pipe size and pipe material. It also remains relatively insensitive to fluid medium inside the pipes, which makes the detection method widely applicable (gas, oil, water pipes, etc). More details follow in the coming sections.

### Radial Pressure Gradient

The detection concept is based on the fact that any leakage in a pipeline alters the pressure and flow field of the working medium. Our group studied, characterized and quantified the phenomenon in detail [17]. The main conclusion is that the region near the leak that is affected is small. However, this region is characterized by a rapid change in static pressure, dropping from $p_{High}$, inside the pipeline, to $p_{Low}$ in the surrounding medium outside (Fig. 2).
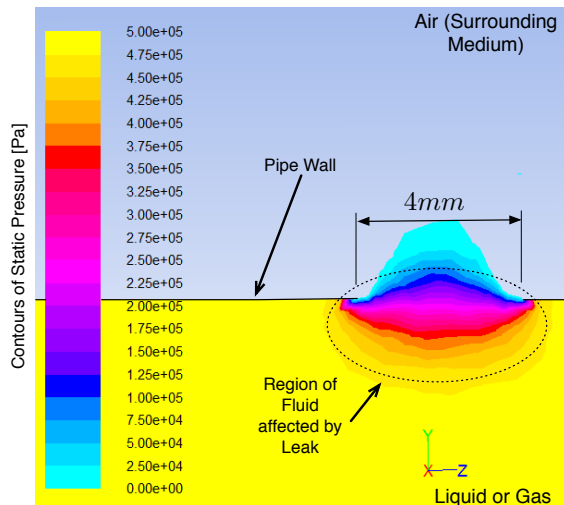
Figure 2. Numerical study of the static pressure distribution in the vicinity of a 4*mm* leak in a water pipe. In this study $\Delta p = 5 bars$. The pipe material/wall is skipped on purpose.
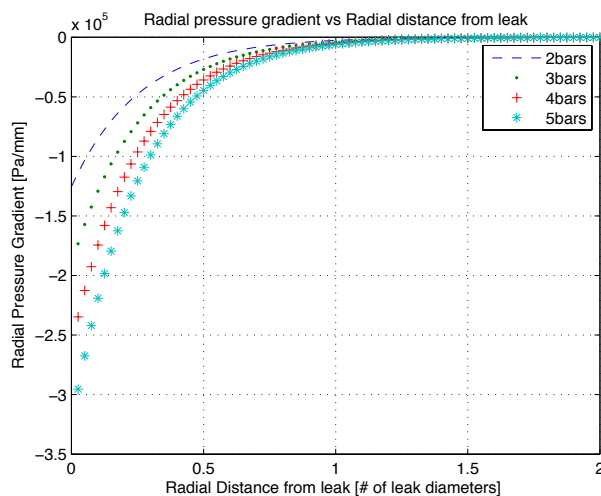


Figure 3. Numerical studies of the radial pressure gradient in the vicinity of a 4*mm* leak. A water pipe of $100mm$ ID was simulated in this case. Different cases for $\Delta p$ are shown.

Let us note the following equation here: $\Delta p = p_{High} - p_{Low}$. This local drop in pressure is the key feature in the proposed leak detection scheme. The rapid change in pressure (radial pressure gradient) due to existence of leaks essentially represents a "suction region". Numerical studies showed that the radial pressure gradient close to the leak is large in magnitude and drops quickly as distance increases. For example in a CFD study of a circular leak of size 2*mm* in diameter within a 100*mm* ID pipe under 2 bars, the radial pressure gradient close to the leak is estimated to be of $O(0.1GPa/m)$. Similar studies are presented in Fig. 3.

Identifying leaks based on this radial pressure gradient proves to be reliable and effective as shown in this paper. Di-

rectly measuring the pressure at each point in order to calculate the gradient is not efficient and should be avoided. However, as a leak can happen at any angle ϕ around the circumference, full observability would require a series of pressure sensors installed around the circumference of the pipe. To avoid the complexity of such an attempt, we introduce a more efficient mechanism to be discussed in the coming section.

**Detector Concept**

In this section we propose a detection concept for the identification of the radial pressure gradient in case of leaks. The main requirement is that the system should be able to detect leaks at any angle ϕ around the circumference of the pipe.

A schematic of the proposed detection concept is shown in Fig. 4. To achieve full observability around the circumference a circular membrane is utilized. The membrane is moving close to the pipe walls at all times complying to diameter changes and other defects on the walls, e.g. accumulated scale. The membrane is suspended by a rigid body, called drum (Fig. 4 [a]). The drum is allowed to rotate about its center point $G$ (about any axis) by design. The latter is allowed by a gimbal mechanism. Details of the design are described in the next section.

In case of a leak the membrane is pulled towards it. This happens because the membrane is pulled by the radial drop in pressure $[\partial p(r)/\partial r]$ described earlier (Fig. 4 [b]). Upon touching the walls, a pressure difference $\Delta p$ is creating the normal force $F$ on the membrane. We can write that:

$$F = \Delta p A_{Leak} \tag{1}$$

where $A_{Leak}$ stands for the cross-sectional area of the leak, which can be of any shape.

As *PipeGuard* continues traveling along the pipe, a new force is generated ($F_z$). This force is a result of friction between the membrane and the pipe walls. $F_z$ is related to the normal force, $F$, by an appropriate friction model, say $F_z = g(F)$. The analytic form of function $g$ is not discussed in this paper. By using Eq. (1) we can see that $F_z$ depends on the pressure difference, since $F_z = g(\Delta p A_{Leak})$.

Then $F_z$ generates an equivalent force and torque on the drum, $M$, a key fact that is discussed further in the coming section. As a result, $M$ forces the drum to rotate about some axis passing through its center, while orientation of the axis depends on the angle ϕ of the leak around the circumference (Fig. 4 [c]). The effects of $M$ can be later sensed by force and/or displacement sensors mounted on the detector. $F_z$ only vanishes when the membrane detaches from the leak and the drum bounces back to the neutral position (Fig. 4 [d]).

In the next section we describe the detailed design of a mechanism that uses the concept presented here to effectively identify leaks in pipes. The proposed system can identify a leak by measuring forces on the drum. Essentially, the problem has
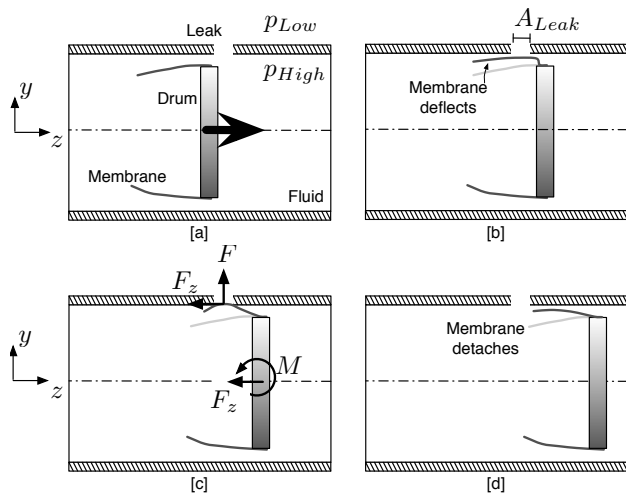
**Figure 4.** The detection concept: [a] "Approach Phase": The detector is moving from left to right with the help of the carrier. Only the drum and the membrane are depicted for simplicity. [b] "Detection Phase A": The membrane is pulled towards the leak due to the suction caused by the drop in pressure. [c] "Detection Phase B": The membrane touches the walls and covers the leak. As *PipeGuard* moves along the pipe a new force, $F_z$ is generated. [d] "Detaching Phase": The membrane detaches from the leak and the drum returns to neutral position.
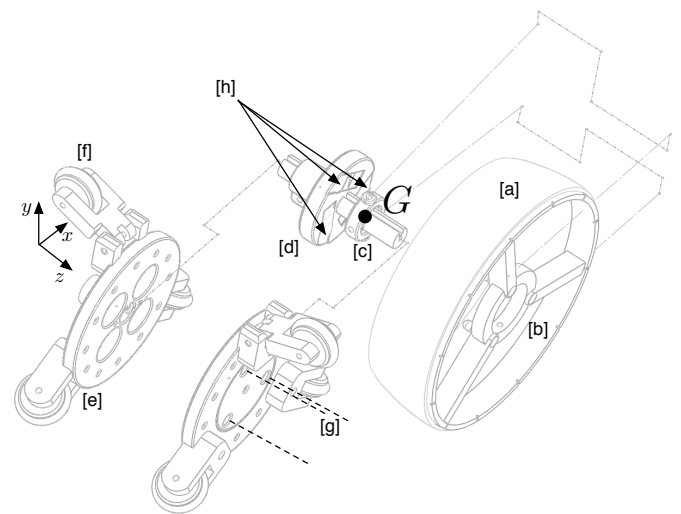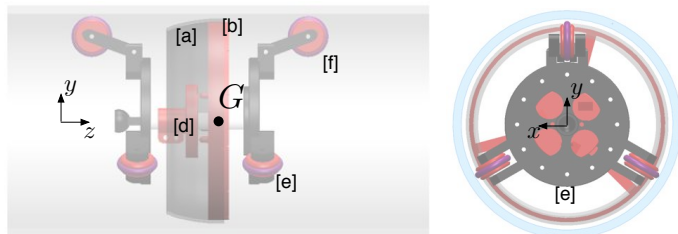


**Figure 5.** 3D solid model of the proposed detector. Side and front view in a pipe. Details: [a] Membrane, [b] Drum, [d] Sensor Chassis and [e] Carrier, [f] Suspension Legs

switched from identifying a radial pressure gradient (at any angle $\phi$), to measuring forces (and/or deflections) on a mechanism.

## Detector Design

A 3D solid model of the proposed detector is shown in Fig. 5. The exploded view of the design is presented in Fig. 6. The drum is depicted in red (solid color) and the membrane in dark grey (transparent color). The drum is suspended by a wheeled system and remains always in the middle of the pipe. A key fact with this proposed design is the gimbal mechanism consisting of two different parts (parts [b] and [c] in Fig. 6). This mechanism allows the drum to pivot about two axes and thus respond to any torque, $M$, about any axis passing through its center point $G$. Moreover, the system dimensions are such that the membrane leaves a small clearance ($< 2mm$) from the walls of the pipe.



**Figure 6.** The exploded view of the proposed design. All key components are laid out. Details: [a] Membrane, [b] Drum, [c] Gimbal, [d] Sensor Chassis, [e] Carrier, [f] Suspension Legs, [g] Axes of Linear Springs, [h] Supporting Points for Drum

Whenever a leak exists, a torque $M$ is generated about some axis on the drum depending on the leak angle, $\phi$, as described earlier. $M$ is sensed by appropriate sensors on the back plate on the carrier. Very small motions on the drum are allowed in this specific embodiment. Springs are used in order to push the drum back to the neutral position after detection is completed (Fig. 4 [d]). In this proposed embodiment three linear springs are used and they are omitted in all figures for simplicity.

## DETECTOR ANALYSIS

In this section we present the forces acting on the drum and justify the placement of sensors on the detector. In addition we propose a detection algorithm for effective leak detection and identification.

### Force Analysis

First we perform a first order statics discussion on the detector. We assume that the drum is only allowed to perform small rotations and, thus, the analysis discussed in this section is only accurate when the motion of the drum is very small and the dynamics are insignificant.

We discussed earlier that a force $\mathbf{F_z} = F_z\hat{\mathbf{e}}_\mathbf{z}$ is generated at leak positions. Here we use $\hat{\mathbf{e}}_\mathbf{z}$ to represent the unit vector along axis $z$ and similar notation will be followed in this section. This force is then generating a torque about point $G$, the center of the gimbal mechanism, which is equal to:

$$\mathbf{M} = F_z R\hat{\mathbf{e}}_\phi$$
$$= F_z R(cos\phi\hat{\mathbf{e}}_\mathbf{y} - sin\phi\hat{\mathbf{e}}_\mathbf{x}) \quad (2)$$
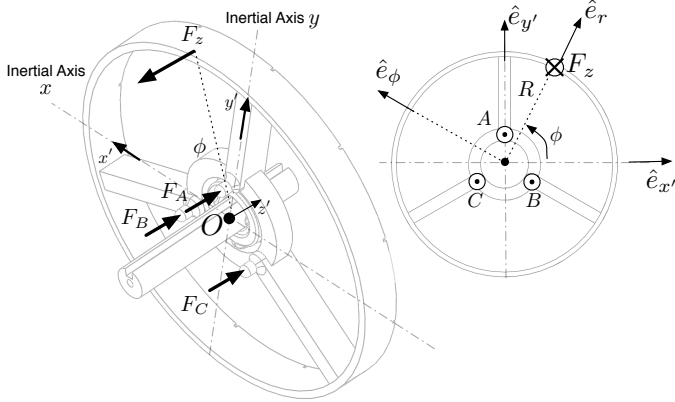
4 Copyright © 2013 by ASME

Figure 7. Forces acting on the drum in case of a leak and a corresponding force $F_z$. A 3D view as well as a front view (side) is shown

The drum is supported by three points, namely points $A$, $B$ and $C$ (Fig. 7). The distance between each of these points and the center of the gimbal $G$ is the same and equal to $r$. We mention at this point that three points of support is the minimal support that is needed to fix the gimbal mechanism in position in such a configuration. In addition, those points are $2\pi/3$ away from each other.

We need to state at this point that the three points do not contribute to the support of the drum at the neutral position. However, when the drum tends to move from neutral position each support creates a corresponding normal force ($\mathbf{F_A}, \mathbf{F_B}, \mathbf{F_C}$) to counterbalance torque $M$ stemming from $F_z$. We can write:

$$\mathbf{M_x} = [F_A r - (F_B + F_C) r \sin(\pi/6)]\hat{\mathbf{e}}_\mathbf{x} \qquad (3)$$

$$\mathbf{M_y} = [F_B - F_C] r \cos(\pi/6)]\hat{\mathbf{e}}_\mathbf{y} \qquad (4)$$

And the total support torque is equal to:

$$\mathbf{M_{support}} = \mathbf{M_x} + \mathbf{M_y} \qquad (5)$$

We assume here that the drum is only allowed to perform small movements and, thus, static analysis is accurate to first order. To complete the analysis we need to equilibrate the torques and forces acting on it. To do this we need to set $\mathbf{M_{support}} = \mathbf{M}$, using Eq. (2,5,3,4).

In addition, since the drum is only allowed to move very little, we can assume that $F_z$ is balanced by the support provided by the axes of the gimbal at point $G$. Then the sum of the three support forces discussed here is approximately equal to zero:

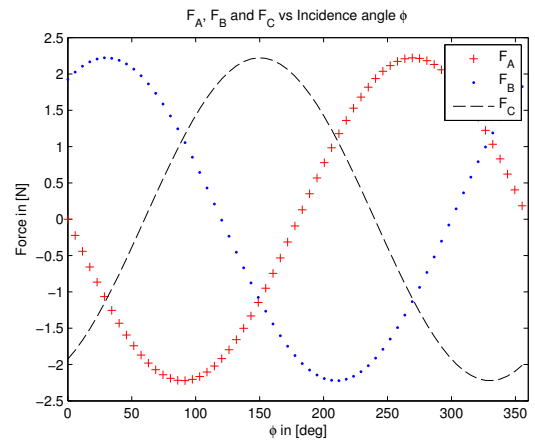$$\mathbf{F_A} + \mathbf{F_B} + \mathbf{F_C} \approx 0 \qquad (6)$$



Figure 8. Forces $F_A, F_B$ and $F_C$ as a function of incidence angle $\phi$. For this case we used $F_z = 1N$, $R = 100/2mm$ and $r = 15mm$.

One can solve the system of equations for the three unknown support forces. Solution to the system of equation gives:

$$\mathbf{F_A} = \frac{-2R\sin\phi}{3r}F_z\hat{\mathbf{e}}_\mathbf{z} \qquad (7)$$

$$\mathbf{F_B} = R\frac{\sin\phi + \sqrt{3}\cos\phi}{3r}F_z\hat{\mathbf{e}}_\mathbf{z} \qquad (8)$$

$$\mathbf{F_C} = R\frac{\sin\phi - \sqrt{3}\cos\phi}{3r}F_z\hat{\mathbf{e}}_\mathbf{z} \qquad (9)$$

We can combine the three forces in a vector, namely : $\mathbf{F} = [\mathbf{F_A F_B F_C}]^\mathbf{T}$. We can write:

$$\begin{aligned} \mathbf{F} &= \mathbf{F}(F_z, \phi) \\ &= \begin{bmatrix} \frac{-2R\sin\phi}{3r}F_z\hat{\mathbf{e}}_\mathbf{z} \\ R\frac{\sin\phi + \sqrt{3}\cos\phi}{3r}F_z\hat{\mathbf{e}}_\mathbf{z} \\ R\frac{\sin\phi - \sqrt{3}\cos\phi}{3r}F_z\hat{\mathbf{e}}_\mathbf{z} \end{bmatrix} \end{aligned} \qquad (10)$$

A plot of these forces as a function of the incidence angle $\phi$ is presented in Fig. 8. In this figure we see that depending on the incidence angle on the circumference of the membrane the signals captured by appropriate force sensors mounted on points $A$, $B$ and/or $C$ are different in magnitude and phase.

For the purpose of this work we built a prototype that is designed to operate in 4" (100$mm$) ID gas pipes and has the following dimensions:

$$R = 47mm$$
$$r = 12.5mm$$

5

Copyright © 2013 by ASME

## Sensor Placement & Algorithm

By installing two force sensors on the supports we are able to measure the corresponding forces directly. The idea here is to measure the support forces as a results of the leak force $F_z$, instead of measuring the leak pressure gradient directly.

To avoid "blind spots" and to be able to detect leaks at any angle around the circumference the system needs to perform at least two force measurements. The latter statement needs to be proven via observability analysis, which is outside the scope of this paper. However, one can think of the simple case of a single leak at $\phi = 0^o$. In such case a force sensor installed on point $A$ would not give any measurement ($F_A = 0$). However, another sensor placed on either point $B$ or $C$ can measure forces due to the leak and can eventually identify it (see Fig. 8).

In this embodiment we install force sensors on points $B$ and $C$ without loss of generality. In addition we propose the use of the following metric in order to effectively trigger alarms in case of leaks:

$$J(t,T) = \int_{t-T}^{t} \sqrt{F_B(\tau)^2 + F_C(\tau)^2}d\tau \qquad (11)$$

where $T$ is the integration period. Whenever $J(t,T) > c$, where $c$ is a predefined constant, a leak is identified. $c$ represents a threshold, above which an alarm is triggered and the existence of a leak is assumed. This quantity needs to be selected in such a way to neglect noise and avoid false alarms. At the same time large values of $c$ will lower the sensitivity of the detection. This metric (Eq. 11) essentially represents a "moving window of integration" of the signal values of the two installed force sensors. This metric proves to be effective in identifying leaks in pipes as shown later in the paper.

## EXPERIMENTAL VALIDATION

In order to validate the concepts developed a prototype that is presented in this section. *PipeGuard* is evaluated in a real gas pipe. Details of the experiments and results are shown at the end of the section.

## PipeGuard's Carrier

For this work *PipeGuard* is designed to operate in 4" (100*mm*) ID gas pipes. However, all concepts discussed in this paper can be scaled and slightly altered accordingly to accommodate pipes of different sizes and perform leak inspection in other fluid media, e.g. water, oil, etc.

In this embodiment *PipeGuard* consists of two modules, namely the carrier and the detector (Fig. 9). The detector design and concepts are discussed in detail in previous sections.

The carrier assures the locomotion of the system inside the pipe. The module is carrying actuators, sensors, power and also electronics for signal processing and communications. A 3D
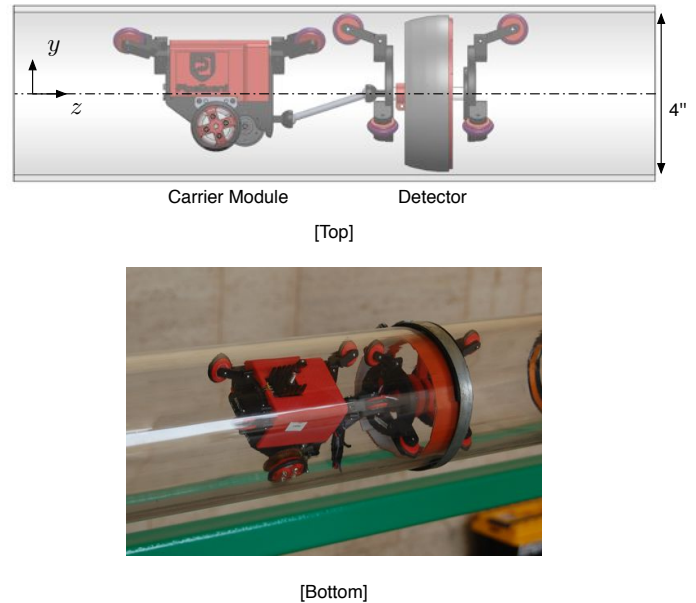


[Top]



[Bottom]

Figure 9. Side view of *PipeGuard*. [Top]: Solid Model. A pipe section (4") is drawn for reference.[Bottom]: The actual developed prototype inside a 4" pipe.
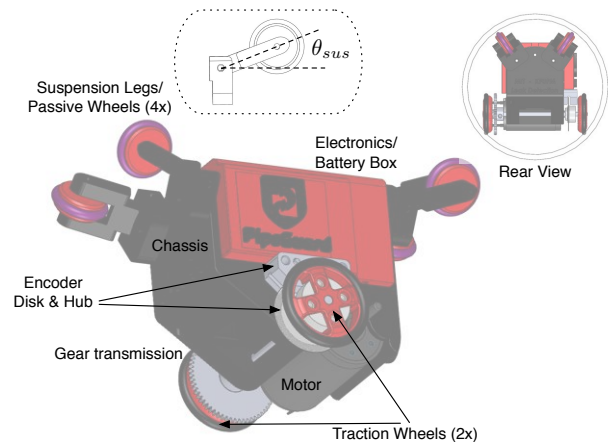


Figure 10. A 3D solid model of the carrier module. A sketch of the carrier's rear view inside a 4" pipe is shown in the top right.

solid model of the carrier with explanations on its main subsystems is presented in Fig. 10.

The module's locomotion is materialized via a pair of traction wheels ($OD = 1\ 3/16''$) (Fig. 10). Those two wheels are touching the lower end of the wall. In addition, the system is suspended by 4 legs with passive wheels from the upper walls as shown in the same figure.

Each suspension wheel has a spring loaded pivot. The angle $\theta_{sus}$ of each pivot point on each suspension wheel is regulated in a passive way and is providing the required compliance to the carrier. That compliance is very important, since it enables the module to align itself properly inside the pipe, over-

6                                                                 Copyright © 2013 by ASME

come misalignments or defects on the pipe walls or even comply with small changes in the pipe diameter.

The main actuator of the module is a 20$W$ brushed DC Motor from "Maxon" (339150). The motor is connected to the traction wheels via a set of gears with ratio 5:1. In order to regulate speed, an incremental rotary encoder (50 counts) from "US Digital" is used and the speed loop is closed. Both disk and hub are shown in Fig. 10. Finally, all electronics, communication modules and batteries are housed inside the carrier module.

## Electronics Architecture

Derived from our design requirements, the robot should be able to perform the following tasks:

– Move and regulate speed in pipes
– Identify leaks by measuring signals from two force sensors at relatively high sampling rates ($f_s > 150Hz$).
– Communicate with the Command Center wirelessly

*PipeGuard's* architecture is developed to meet these requirements and is shown in Fig. 11. To perform the aforementioned tasks two micro-controllers are used. Micro-controller #1 is dedicated to speed regulation and micro-controller #2 is performing real-time leak sensing.

The workflow is the following: The user specifies a motion command on the computer. The computer sends out the motion command including desired speed and desired position to *PipeGuard*. After the WiFi transceiver on the robot receives the command, it delivers the command to micro-controller #2. Micro-controller #2 performs closed loop speed control in order to regulate speed of the carrier. At the same time it calculates speed (by measuring the signal from the encoder) and commands the system to stop if it reaches the end of the pipe section (or any other point along the pipe as specified by the operator).

Parallel to micro-controller #2, micro-controller #1 is responsible for leak detection and for sending out sensor data to the WiFi transceiver. This micro-controller receives signals from the two force sensors installed on the detector. At the same time it receives the measured position from the encoder mounted on the carrier. It compiles the correlated force sensor data with position data and sends them out through the WiFi transceiver. The WiFi receiver on the command center then receives the data, decomposes them and supplies them to the user via the graphical user interface on the computer.

In this embodiment of *PipeGuard*, the WiFi transceiver selected is an Xbee Pro 900MHz RF module. We use two Arduino Pro Mini 328 5V/16MHz and the motor driver under codename VNH5019 from Polulu. The whole system is powered by a 11.1V 350 mAh 65C Li-polymer battery. Finally, we use two FSR 400 force sensors for leak detection from "Interlink Electronics". The latter ones are powered at 5V and a resistor of 8$k\Omega$ is used for the necessary voltage division. The whole system (Carrier and Detector) can run for 30mins with this configuration, performing leak inspection and locomotion inside pipelines.
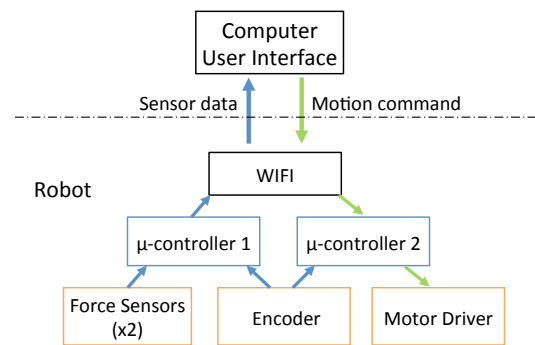


Figure 11. High level system architecture of *PipeGuard*. Two micro-controllers are installed on the system for simultaneous speed regulation and leak detection.

## Experimentation

In this section we evaluate *PipeGuard* in an experimental setup we built in our lab. The setup consists of a straight 4" ID and 1.40$m$ long PVC pipe. The system is deployed in the pipe and performs leak detection in a pressurized air environment. Artificial leaks have been created on the pipe walls in the shape of circular 2$mm$ openings. Those openings can be considered small for the general case and such small leaks fail to be detected by most state-of-the-art systems available.

A picture of *PipeGuard* inside the experimental setup is shown in Fig. 12. *PipeGuard* moves along the pipe from [Start] to [End] and its job is to identify the leaks. In Fig. 12 leak #1 is covered and leak #2 is opened.

**Low Speed Detection** Initially we let the system run in the pipe at low speeds. We command *PipeGuard* to move at $\omega_d = 2Hz$, which is equivalent to $v_d = 0.19m/s$. At this speed the system is able to traverse the distance from [Start] to [End] in approximately 5$sec$. The signals captured by the two force sensors are shown in Fig. 13. A clear change in the signals reveals the existence of a leak in the pipe. Note here that for this experiment the line pressure was selected to be equal to 15$psi$. In the same figure the evolution of the proposed metric from Eq. 11 is shown. A clear peak above the noise level is indicating the existence of a leak at $t = t^*$ when $J(t^*, T = 0.2sec) > 0.025$.

As *PipeGuard* approaches the leak, the signals from the two force sensors do not show any large variations from the DC value. Noise can occur but is much smaller in amplitude than the leak signal (Fig. 13). Detection occurs in four phases. Initially *PipeGuard* approaches the leak. Then the membrane is moving towards the leak because of the effect of the radial pressure gradient. The latter small movement results in a small change in the signals (undershoot in this case). Afterwards and when the membrane touches the wall at the leak position a force $F_z$ is generated, resulting in the torque $M$ on the drum. The latter torque pushes the drum to move and thus, signals of the two sensors
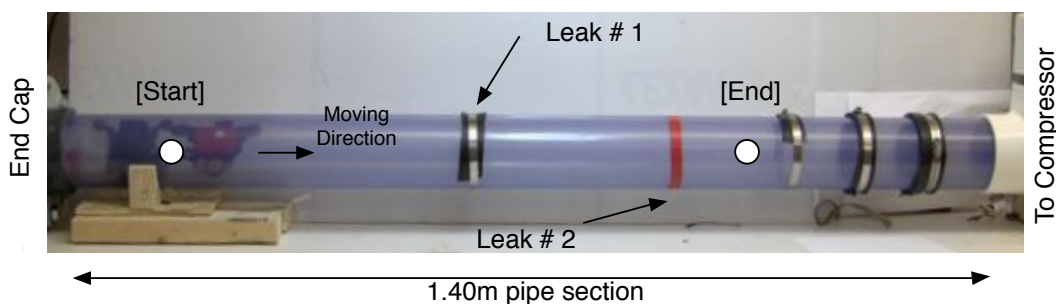
Figure 12. The experimental setup we used for the evaluation of *PipeGuard*. The system moves along the pipe from ⌈Start⌋ to ⌈End⌋ and performs leak detection. Along this path there are two potential leaks to be detected. In this specific picture leak #1 is covered and closed, while leak #2 is open and can be detected.
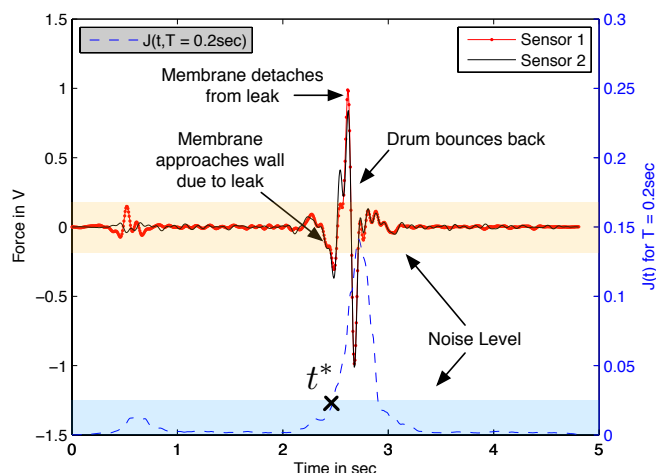


Figure 13. Sensor signals as *PipeGuard* moves along the pipe. Signals presented here are collected at 160Hz for each sensor. Line pressure is equal to $15psi$. In addition the metric $J(t, T = 0.2sec)$ is plotted here. Leak is successfully identified.
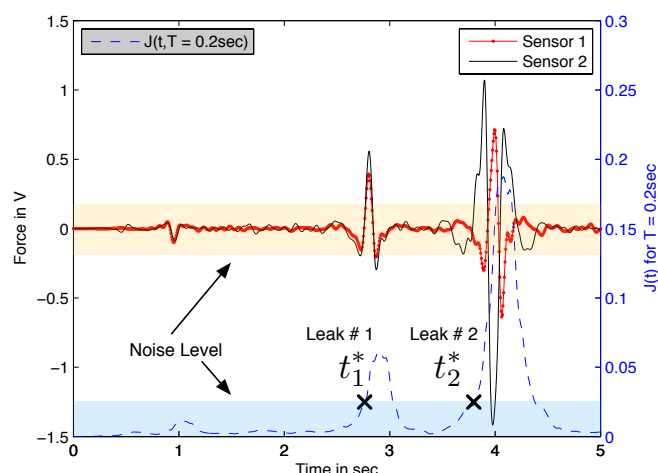


Figure 14. Sensor signals as *PipeGuard* moves along the pipe. Signals presented here are collected at 160Hz for each sensor. Line pressure (at the compressor) is equal to $20psi$. Sensor signals are in phase for leak #1 and out of phase for leak #2. In addition the metric $J(t, T = 0.2sec)$ is plotted here. Two leaks is successfully identified.

change significantly. Signals continue to increase up to a certain point when the membrane detaches from the leak. At this point the drum bounces back to the neutral position and signals return to their nominal (zero) values.

Successful detection is performed when both leaks along the pipe are opened. Again *PipeGuard* is commanded to move at $v_d = 0.19m/s$. The detector passes by the two consecutive leaks and the signals captured are presented in Fig. 14. Signal magnitude for leak #1 is smaller than the magnitude for leak #2. This is expected, as line pressure at the position of leak #1 is reduced, because of the existence of leak #2. By carefully selecting corresponding thresholds $c$, one can trigger alarms at times $t_i^*$ when $J(t_i^*, T) > c$. In this case, again, $c = 0.025$ is selected in order to avoid false alarm (neglect noise) and effectively trigger alarms at leak locations.

By carefully observing Fig. 14 we can see that signals cap-

tured as *PipeGuard* is passing by the first leak are in phase, while the signals at the second leak are out of phase. This occurs because the two leaks are at a different position on the circumference of the pipe ($\phi_1 \neq \phi_2$). By designing appropriate algorithms one can estimate the position of the leak on the circumference, but such discussion is outside the scope of this paper.

**High Speed Detection** This specific version of *PipeGuard* is able to move inside the pipes at relatively high speeds. Experimentation showed that *PipeGuard's* motor is saturated at approximately $\omega_d = 9.23Hz$, which is equivalent to $v_d = 0.875m/s$. At this speed *PipeGuard* is able to inspect pipes at a rate of more than $3km$ per hour.

Even at these speeds *PipeGuard* is still able to inspect

8                                                    Copyright © 2013 by ASME
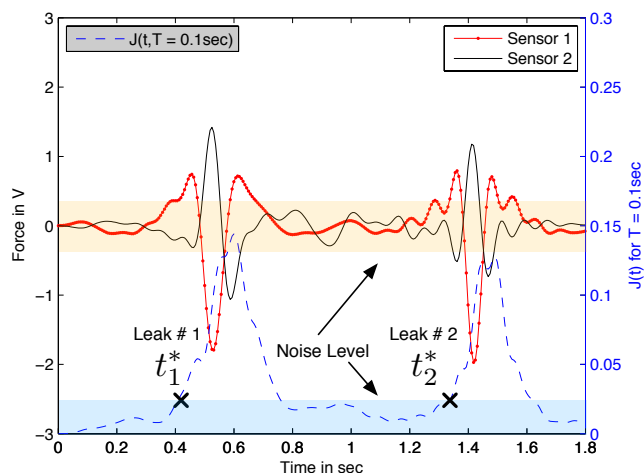
Figure 15. Sensor signals as *PipeGuard* moves along the pipe. Signals presented here are collected at 160Hz for each sensor. Line pressure (at the compressor) is equal to $20psi$. *PipeGuard* is moving at approximately $0.875m/s$ inside the pipe. In addition the metric $J(t, T = 0.1sec)$ is plotted here. Two leaks are successfully identified.

pipelines and detect leaks in a very reliable fashion. By carefully selecting the triggering thresholds one is able to trigger alarms only when leaks are present and avoid false alarms. Example leak signals captured at those high speeds are shown in Fig. 15. In this case noise magnitude is higher, but still leak signals stand out significantly. In this case $c = 0.025$, but one would probably try to increase threshold. The latter would enable the sensor to neglect higher noise levels at the cost of reducing the sensitivity of the detection.

## CONCLUSIONS AND FUTURE WORK

In this paper a new system for the detection of leaks in pipes is proposed. *PipeGuard* is able to inspect leaks in an autonomous and reliable fashion. *PipeGuard's* detector is based on a pressure gradient in the vicinity of the leak as discussed throughout this paper. By utilizing this local phenomenon a smart and reliable detector is built, a minimum amount of sensors are used and the system is validated through experiments. A metric to quantify leak signals and trigger alarms at leak locations is proposed and proves to be effective. False alarms can be avoided by carefully adjusting the triggering thresholds before deployment of the robot inside pipes. Finally, the detector is sensitive enough to identify small leaks at low pressures as proven in the experimental section of the paper. Numerical and experimental work showed that the same concepts can be extrapolated to water applications and are not restricted to gas pipes.

Our future work includes the refinement and optimization of the design of the detector. We plan to continue working on this technology for both gas and water applications and maybe also other types of liquids. Since experimentation was restricted to

straight pipelines thus far, we plan to conduct extensive tests in different environments and pipe configurations.

## REFERENCES

[1] Mays L., 2000. *Water Distribution Systems Handbook*. McGraw-Hill.

[2] Hunaidi O., Chu W., Wang A. and Guan W., 1999. "Leak detection method for plastic water distribution pipes". *Advancing the Science of Water, Fort Lauderdale Technology Transfer Conference, AWWA Research Foundation*, pp. 249–270.

[3] Fuchs H. V. and Riehle R., 1991. "Ten years of experience with leak detection by acoustic signal analysis". *Applied Acoustics,* **33**, pp. 1–19.

[4] Hunaidi O. and Chu W., 1999. "Acoustical characteristics of leak signals in plastic water distribution pipes". *Applied Acoustics,* **58**, pp. 235–254.

[5] Bracken M. and Hunaidi O., 2005. "Practical aspects of acoustical leak location on plastic and large diameter pipe". *Leakage 2005 Conference Proceedings*(448-452).

[6] Hunaidi O., Chu W., Wang A. and Guan W., 2000. "Detecting leaks in plastic pipes". *Journal - American Water Works Association,* **92**(2), pp. 82–94.

[7] Hunaidi O. and Giamou P., 1998. "Ground-penetrating radar for detection of leaks in buried plastic water distribution pipes". *Seventh International Conference on Ground Penetrating Radar (GPR'98)*, pp. 783–786.

[8] Kurtz D. W., 2006. "Developments in a free-swimming acoustic leak detection system for water transmission pipelines". *ASCE Conf. Proc.,* **25**(211).

[9] Bond A., Mergelas B. and Jones C., 2004. "Pinpointing leaks in water transmission mains". *ASCE Conf. Proc.,* **91**(146).

[10] Chatzigeorgiou D., Youcef-Toumi K., Khalifa A. and Ben-Mansour R., 2011. "Analysis and design of an in-pipe system for water leak detection". *ASME International Design Engineering Technical Conferences & Design Automation Conference (IDETC/DAC2011)*.

[11] Khalifa A., Chatzigeorgiou D., Youcef-Toumi K., Khulief Y. and Ben-Mansour R., 2010. "Quantifying acoustic and pressure sensing for in-pipe leak detection". *ASME Inter-*

9

Copyright © 2013 by ASME

*national Mechanical Engineering Congress & Exposition (IMECE2010).*

[12] Chatzigeorgiou D., Khalifa A., Youcef-Toumi K. and Ben-Mansour R., 2011. "An in-pipe leak detection sensor: Sensing capabilities and evaluation". *ASME/IEEE International Conference on Mechatronic and Embedded Systems and Applications (MESA2011).*

[13] Choi H-R. and Roh S-G, 2005. "Differential-drive in-pipe robot for moving inside urban gas pipelines". *Transactions on Robotics,* **21**(1).

[14] Schempf H., Mutschler E., Goltsberg V., Skoptsov G., Gavaert A. and Vradis G., 2003. "Explorer: Untethered real-time gas main assessment robot system". *Proc. of Int. Workshop on Advances in Service Robotics (ASER).*

[15] Mirats Tur, J. M., and Garthwaite, W., 2010. "Robotic devices for water main in-pipe inspection: A survey". *Journal of Field Robotics,* **27**(4), pp. 491–508.

[16] Wu D., Youcef-Toumi K., Mekid S. Ben Mansour R., 2013. "Relay node placement in wireless sensor networks for pipeline inspection". *IEEE American Control Conference (ACC2013).*

[17] Ben-Mansour R, M.A. Habib, A. Khalifa, K. Youcef-Toumi and D. Chatzigeorgiou, 2012. "A computational fluid dynamic simulation of small leaks in water pipelines for direct leak pressure transduction". *Computer and Fluids*, p. doi:10.1016/j.compfluid.2011.12.016.